HPat provides a link between deadenylation and decapping in metazoa

Gabrielle Haas, Joerg E. Braun, Cátia Igreja, Felix Tritschler, Tadashi Nishihara, and Elisa Izaurralde

Max Planck Institute for Developmental Biology, D-72076 Tübingen, Germany

THE JOURNAL OF CELL BIOLOGY

Decapping of eukaryotic messenger RNAs (mRNAs) occurs after they have undergone deadenylation, but how these processes are coordinated is poorly understood. In this study, we report that *Drosophila melanogaster* HPat (homologue of Pat1), a conserved decapping activator, interacts with additional decapping factors (e.g., Me31B, the LSm1–7 complex, and the decapping enzyme DCP2) and with components of the CCR4–NOT deadenylase complex. Accordingly, HPat triggers deadenylation and decapping when artificially tethered to an mRNA reporter. These activities reside, unexpectedly, in a proline-rich region. However, this region alone cannot restore decapping in cells depleted of endogenous HPat but also requires the middle (Mid) and the very C-terminal domains of HPat. We further show that the Mid and C-terminal domains mediate HPat recruitment to target mRNAs. Our results reveal an unprecedented role for the proline-rich region and the C-terminal domain of metazoan HPat in mRNA decapping and suggest that HPat is a component of the cellular mechanism that couples decapping to deadenylation in vivo.

Introduction

Eukaryotic mRNAs are degraded by two alternative pathways, both of which are initiated by a gradual shortening of the poly(A) tail by deadenylation. In one, the 3′ to 5′ decay pathway, the poly(A) tail is first removed, and then the exosome and cofactors digest the mRNA exonucleolytically from the 3′ end (Houseley et al., 2006). In the other, the 5′ to 3′ decay pathway, deadenylation is followed by the removal of the 5′ cap structure by the decapping enzyme DCP2; decapped mRNA is then susceptible to 5′ to 3′ exonucleolytic degradation by XRN1 (Bail and Kiledjian, 2006; Simon et al., 2006).

The decapping enzyme DCP2 requires additional proteins for full activity and/or stability (Bail and Kiledjian, 2006; Simon et al., 2006). Proteins that enhance decapping in *Saccharomyces cerevisiae* include DCP1, EDC1–3 (enhancer of decapping 1, 2, and 3), the heptameric LSm1–7 complex, Dhh1 (DExH/D-box RNA helicase 1; Me31B in *Drosophila melanogaster*), and Pat1 (HPat in *D. melanogaster*). With the exception of EDC1 and -2, these proteins are conserved, yet most are not functionally characterized in multicellular eukaryotes.

In *S. cerevisiae*, Pat1 interacts with the Lsm1–7 complex and Dhh1 (Bonnerot et al., 2000; Bouvert et al., 2000;

Fromont-Racine et al., 2000; Tharun et al., 2000; Coller et al., 2001; Tharun and Parker, 2001; Fischer and Weis, 2002). The Pat1–LSm1–7 complex preferentially binds to the 3′ ends of oligoadenylated mRNAs that have undergone deadenylation, thereby protecting them from 3′ trimming and further degradation (He and Parker, 2001; Tharun and Parker, 2001; Chowdhury et al., 2007; Chowdhury and Tharun, 2008, 2009). This complex then activates decapping, most likely by recruiting additional decapping activators and the decapping enzyme DCP2 (Hatfield et al., 1996; Bouvert et al., 2000; He and Parker, 2001; Chowdhury et al., 2007; Decker et al., 2007; Chowdhury and Tharun, 2008, 2009; Pilkington and Parker, 2008; Tharun, 2009). Pat1 also associates with DCP1, DCP2, and EDC3 in yeast, which is consistent with a role in decapping (Fromont-Racine et al., 2000; Tharun et al., 2000; Tharun and Parker, 2001; Pilkington and Parker, 2008). Additionally, Pat1 and the LSm1–7 complex copurify with Xrn1 (Bouvert et al., 2000), suggesting a possible role for Pat in coupling decapping to 5′ to 3′ mRNA degradation.

Like many components of the 5′ to 3′ mRNA decay pathway, Pat1 localizes to P bodies and, moreover, is required

Correspondence to Elisa Izaurralde: elisa.izaurralde@tuebingen.mpg.de

Abbreviations used in this paper: dsRNA, double-stranded RNA; F-Luc, firefly luciferase; IP, immunoprecipitation; MBP, maltose-binding protein; Mid, middle; R-Luc, *Renilla* luciferase; RT-qPCR, quantitative RT-PCR; Tral, trailer hitch.

for P-body integrity (Pilkington and Parker, 2008). A fraction of Pat1 is also found in polysomes (Bonnerot et al., 2000; Wyers et al., 2000), suggesting that it associates with actively translated mRNAs and may commit them to degradation in response to a triggering signal (Bonnerot et al., 2000). Intriguingly, Pat1 was reported to play dual roles in translation: it stimulates translation initiation (Wyers et al., 2000) but is also required for general translational repression during glucose deprivation (Coller and Parker, 2005). Furthermore, Pat1 overexpression can repress translation and cause mRNAs to accumulate in P bodies (Coller and Parker, 2005). These and additional studies suggest that Pat1 is a key regulator in the transition of mRNAs from a translationally active state associated with polysomes to a ribosome-free translationally repressed state that commits the mRNA to degradation (Coller and Parker, 2005; Pilkington and Parker, 2008). In this repressed state, mRNAs may aggregate into P bodies (Coller and Parker, 2005).

Pat1 is conserved in eukaryotes, and Pat1 orthologues in *D. melanogaster* and human cells (HPat and PatL1, respectively) localize to P bodies (Eulalio et al., 2007a; Scheller et al., 2007). The role of metazoan Pat1 orthologues in decapping is also conserved, as suggested by the observation that codepletion of HPat and Me31B strongly inhibits decapping triggered by microRNAs or by tethered GW182 in *D. melanogaster* cells (Eulalio et al., 2007c). Nonetheless, the interactions of Pat1 orthologues with additional decapping activators and the role of Pat1 orthologues in decapping remain largely unknown in multicellular eukaryotes.

Pat1 proteins are characterized by a conserved N-terminal sequence, a proline-rich region, a middle (Mid) domain, and a C-terminal domain (termed Pat-C). A study in *S. cerevisiae* showed that the Pat1 Mid domain interacts with the LSm1–7 ring and is essential for decapping in vivo (Pilkington and Parker, 2008). Sequences located N- or C-terminally to the Mid domain stimulate but are not required for decapping. Furthermore, Pat-C is required for Pat1 to localize to P bodies and confers the interaction with DCP1, EDC3, and RNA (Pilkington and Parker, 2008).

In this study, we analyzed HPat interactions and function in *D. melanogaster* using coimmunoprecipitation (co-IP) and complementation assays. In addition to the interaction between HPat and Me31B, DCP2 or the LSm1–7 complex, which are conserved in yeast, our study revealed that HPat interacts with the CCR4–NOT deadenylase complex. These findings suggest that HPat plays a role in coupling decapping to deadenylation. Accordingly, we observed that HPat promotes deadenylation and decapping of mRNAs in tethering assays. Unexpectedly, these activities are mediated by a proline-rich region, which we show is also required for P-body integrity. However, in contrast to results in yeast, we show that in addition to the Mid domain, both the proline-rich region and Pat-C are required to restore decapping in cells depleted of endogenous HPat. Our findings reveal that yeast and *D. melanogaster* differ significantly as to which HPat domains are required for decapping, highlighting the importance of characterizing decapping complexes in metazoa.

Results

HPat coimmunoprecipitates Me31B, DCP2, and the LSm1–7 complex

To systematically investigate the network of interactions between HPat and decapping activators in metazoa, we coexpressed HA-, V5-, or GFP-tagged versions of these proteins in *D. melanogaster* S2 cells and used anti-HA antibodies to coimmunoprecipitate V5- or GFP-tagged proteins from cell lysates. We used this method to detect interactions with DCP1, DCP2, EDC3, EDC4, Me31B, Tral (trailer hitch), XRN1, and components of the LSm1–7 complex.

HPat coimmunoprecipitated with Me31B but not with DCP1, EDC3, or Tral (Fig. 1 A, lanes 7–10). Both EDC3 and Tral interact directly with Me31B (Tritschler et al., 2009), suggesting that the interaction of HPat with Me31B mutually excludes an interaction with Me31B–EDC3 or Me31B–Tral (see Figs. 3 and 4). When coexpressed in *Escherichia coli*, recombinant protein fragments of HPat and Me31B interact, showing the proteins bind each other directly (unpublished data).

In yeast, Pat1 associates with the LSm1–7 complex (Bonnerot et al., 2000; Bouveret et al., 2000; Fromont-Racine et al., 2000; Tharun et al., 2000; Tharun and Parker, 2001). Accordingly, we observed that HPat coimmunoprecipitated LSm1, -3, and -7 (Fig. 1 B). HPat interaction with LSm1 was insensitive to RNase A treatment (Fig. S1 A), suggesting that it is not mediated by RNA. LSm1 and -7 also coimmunoprecipitated with Me31B but not with any of the other proteins tested (Fig. 1 C; Tritschler et al., 2007, 2008). Finally, we observed that HPat coimmunoprecipitated DCP2 in an RNA-independent manner but not XRN1 or EDC4 (Fig. 1 D; Fig. S1, B and C; and not depicted). Thus, in addition to the interactions with Me31B and the LSm1–7 ring, which are conserved in *S. cerevisiae*, we detected an RNase A–insensitive interaction between HPat and DCP2. In contrast to our findings in this study, this interaction is sensitive to RNase A treatment in yeast (Tharun and Parker, 2001).

Me31B binds to the conserved N-terminal sequence of HPat

The interaction of HPat with Me31B is conserved in *S. cerevisiae* (Coller et al., 2001; Fischer and Weis, 2002). Despite conservation, the protein domains involved in this interaction were not defined. To identify them, we performed co-IP assays using different HPat and Me31B deletion mutants. Pat1 orthologues are characterized by a conserved N-terminal sequence of ∼50 residues, a proline-rich region, a Mid domain, and a C-terminal domain termed Pat-C (Fig. 2, A and B). The boundary between the Mid domain and Pat-C was chosen on the basis of sequence alignments between Pat1 orthologues from various species.

We observed that Me31B interacted only with an N-terminal fragment of HPat (residues 1–499) but not with a construct comprising the Mid domain and Pat-C (Fig. 2 C, lanes 8 and 9). The N-terminal fragment contains the conserved N-terminal sequence (residues 1–56; Fig. 2 B) and the proline-rich region (13.6%), which is particularly long in the *D. melanogaster* protein and also rich in glutamine residues (16%; Fig. 2 A,
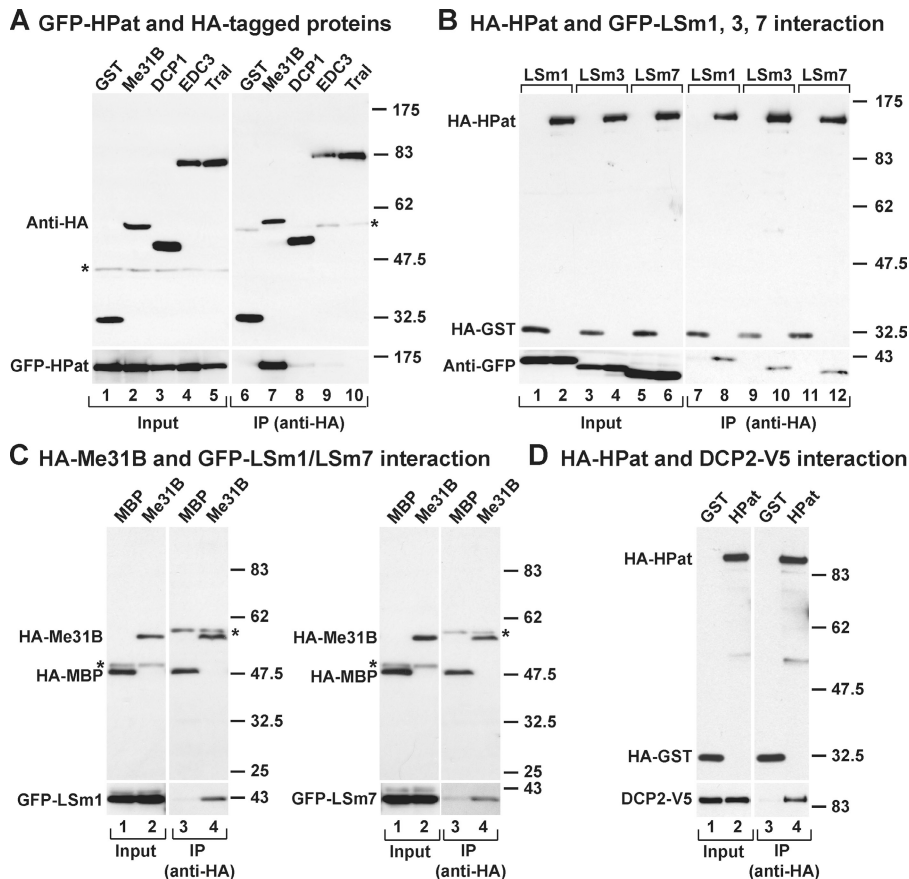
A GFP-HPat and HA-tagged proteins

GST Me31B DCP1 EDC3 Tral GST Me31B DCP1 EDC3 Tral

— 175
— 83

Anti-HA

— 62
— * (47.5 region)
— 47.5
*
— 32.5

GFP-HPat — 175

1 2 3 4 5 6 7 8 9 10

Input IP (anti-HA)

B HA-HPat and GFP-LSm1, 3, 7 interaction

LSm1 LSm3 LSm7 LSm1 LSm3 LSm7

HA-HPat

— 175
— 83
— 62
— 47.5

HA-GST

— 32.5

Anti-GFP

— 43

1 2 3 4 5 6 7 8 9 10 11 12

Input IP (anti-HA)

Figure 1. **HPat coimmunoprecipitates DCP2, Me31B, and the LSm1–7 complex.** (A–D) GFP-, V5-, and HA-tagged proteins were coexpressed in S2 cells as indicated. Cell lysates were immunoprecipitated using a monoclonal anti-HA antibody. HA-tagged versions of GST or MBP served as negative controls. Inputs (1%) and immunoprecipitates (10%) were analyzed by Western blotting. In D, 30% of the IP fraction was loaded. Asterisks indicate cross-reactivity of the primary antibodies with an endogenous protein (input panels) or of the secondary antibody with the immunoglobulin heavy chain (IP panels). Molecular mass is indicated in kilodaltons.

C HA-Me31B and GFP-LSm1/LSm7 interaction

MBP Me31B MBP Me31B

— 83
— 62

HA-Me31B *

HA-MBP *

— 47.5
— 32.5
— 25

GFP-LSm1 — 43

1 2 3 4

Input IP (anti-HA)

MBP Me31B MBP Me31B

— 83
— 62

HA-Me31B *

HA-MBP *

— 47.5
— 32.5
— 25

GFP-LSm7 — 43

1 2 3 4

Input IP (anti-HA)

D HA-HPat and DCP2-V5 interaction

GST HPat GST HPat

HA-HPat

— 83
— 62
— 47.5

HA-GST — 32.5

DCP2-V5 — 83

1 2 3 4

Input IP (anti-HA)

P-rich region). Because the interaction of HPat with Me31B is conserved, we hypothesized it could be mediated by the conserved N-terminal sequence. Indeed, we observed that an HPat protein lacking the N-terminal sequence did not interact with Me31B (Fig. 2 C, lane 10). Conversely, a protein fragment comprising only the conserved N-terminal sequence was sufficient for the interaction with Me31B (Fig. 2 D, lane 9). Thus, the conserved N-terminal sequence represents the Me31B-binding site in HPat.

HPat, EDC3, or Tral assembles with Me31B into distinct protein complexes

Me31B is a DEAD-box helicase and, like all members of this protein family, consists of two RecA-like domains (Fig. 3 A). Previously, we showed that the C-terminal RecA-like domain interacts in a mutually exclusive manner with the FDF motifs of EDC3 and Tral (Tritschler et al., 2008, 2009). Surprisingly, in this study, we could also detect an interaction between the Me31B C-terminal RecA-like domain and full-length HPat (Fig. 3 B, lane 8) or with the HPat conserved N-terminal sequence (Fig. 2 D, lane 12). However, HPat did not interact with EDC3 or Tral (Fig. 1 A), suggesting that HPat, EDC3, and Tral may form mutually exclusive interactions with Me31B.

To investigate this possibility further, we cotransfected S2 cells with mixtures of plasmids encoding three proteins: EDC3 (or Tral), HPat, and Me31B. We used three different mixtures, each containing a plasmid expressing one HA-tagged and two GFP-tagged proteins. We then assayed whether the proteins

fused to GFP could be coimmunoprecipitated from cell lysates using anti-HA antibodies. We observed that HA-Me31B coimmunoprecipitated GFP-HPat and -EDC3, showing that Me31B does indeed interact with both proteins (Fig. 3 C, lanes 8–10). In contrast, HA-HPat coimmunoprecipitated GFP-Me31B but not GFP-EDC3 (Fig. 3 D, lanes 8–10), whereas HA-EDC3 coimmunoprecipitated GFP-Me31B but not GFP-HPat (Fig. 3 E, lanes 8–10). Similar results were obtained when EDC3 was substituted by Tral in the co-IP assays (Fig. S2), suggesting that Me31B associates with HPat, Tral, and EDC3 to form distinct protein complexes.

EDC3 competes with HPat for binding to Me31B

The crystal structure of RCK (human Me31B orthologue) in complex with the FDF motif of EDC3 revealed surface residues on RCK (or Me31B) that are critical for the interaction with EDC3 and Tral (Tritschler et al., 2009). To determine whether HPat competes with EDC3 and Tral for this same binding surface, we tested whether an Me31B mutant that does not interact with EDC3 (or Tral) could still bind HPat. Specifically, we took advantage of an Me31B (Mut1) mutated at four surface residues involved in the interaction with the FDF motifs of EDC3 and Tral. We also tested an Me31B mutant (Mut2) that interacts with Tral but not with EDC3 (Tritschler et al., 2009). In IP assays, the two Me31B mutants interacted with HPat (Fig. 4 A, lanes 8–10), whereas Me31B-Mut1 did not interact with EDC3 as expected (Fig. 4 A, lane 12).
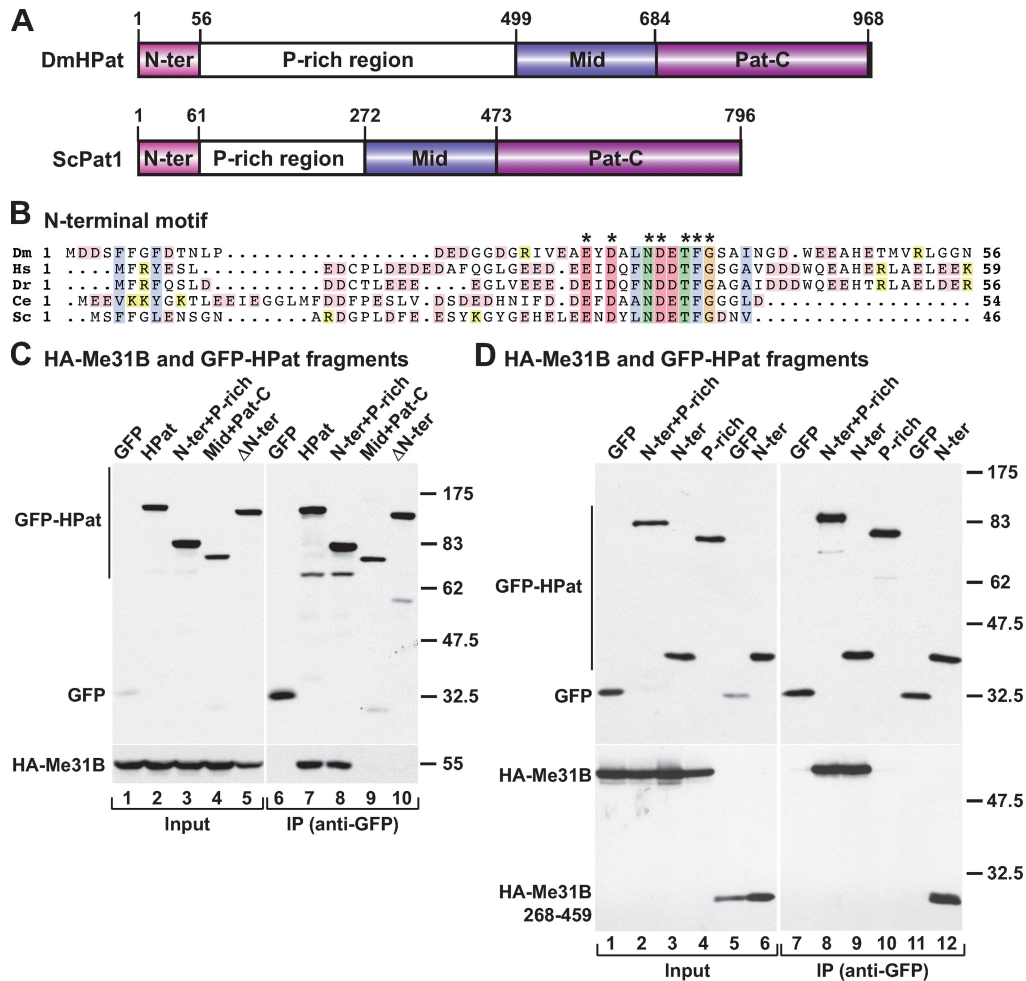
Figure 2. **The N-terminal conserved sequence mediates HPat interaction with Me31B.** (A) Domain organization of HPat. HPat proteins contain a conserved N-terminal (N-ter) sequence, a glutamine/proline-rich region (P-rich), a Mid domain, and Pat-C. Numbers above the protein outline represent amino acid positions at fragment boundaries for the *D. melanogaster* protein. *S. cerevisiae* Pat1 is shown for comparison. (B) Sequence alignment of the N-terminal conserved sequence of Pat1 orthologues from *Homo sapiens* (Hs), *Danio rerio* (Dr), *D. melanogaster* (Dm), *Caenorhabditis elegans* (Ce), and *S. cerevisiae* (Sc). Asterisks indicate invariant residues. Hydrophobic, polar, and acidic residues are shaded in blue, green and magenta, respectively. Glycines are shaded orange. Unconserved acidic and basic residues are shaded light magenta and yellow, respectively. (C and D) Interaction between full-length GFP-HPat or HPat fragments with full-length Me31B or its C-terminal RecA-like domain. Cell lysates were immunoprecipitated and analyzed as described in Fig. 1. Molecular mass is indicated in kilodaltons.

Our results indicate that HPat binds to Me31B via surface residues different than those contacting EDC3 (or Tral); yet, the Me31B interaction with HPat and EDC3 (or Tral) appears to be mutually exclusive, suggesting that the binding surfaces partially overlap. Alternatively, EDC3 (or Tral) may interfere with HPat binding as the result of steric hindrance.

To further investigate whether EDC3, Tral, and HPat form mutually exclusive interactions with Me31B, we performed competition assays. In these assays, we tested whether a peptide containing the Me31B-binding domain of EDC3 (i.e., the FDF motif) competed with HPat for binding to Me31B when added to cell lysates before IP. Indeed, the peptide did interfere with HPat binding to Me31B, as expected for a mutually exclusive interaction (Fig. 4 B, lanes 9 and 10). As a control, we tested the corresponding peptide carrying alanine substitutions of the phenylalanine residues in the EDC3-FDF motif (ADA peptide); this peptide no longer binds Me31B and had no effect (Fig. 4 B, lanes 11 and 12; Tritschler et al., 2009). Because the EDC3-FDF

peptide also competes with Tral for binding to Me31B (Tritschler et al., 2009), we conclude that HPat, EDC3, and Tral interact with Me31B in a mutually exclusive manner.

The Mid domain of HPat confers interaction with the LSm1–7 complex

Next, we tested which HPat domains can interact with LSm1 and DCP2. We observed that a fragment of HPat containing the Mid domain plus Pat-C (residues 500–968) was necessary and sufficient to interact with both LSm1 and DCP2 (Fig. 5, A–D). When the Mid domain and Pat-C were tested individually, we observed that both LSm1 and DCP2 interacted with the Mid domain but not with Pat-C (Fig. 5, B and D). However, the interaction of DCP2 with the Mid domain was less efficient than with the fragment also containing Pat-C, suggesting that Pat-C contributes to DCP2 binding. These results, together with the observation that DCP2 does not interact with LSm1 (Fig. S1 D), suggest that DCP2 binds HPat independently of the LSm1–7 ring.
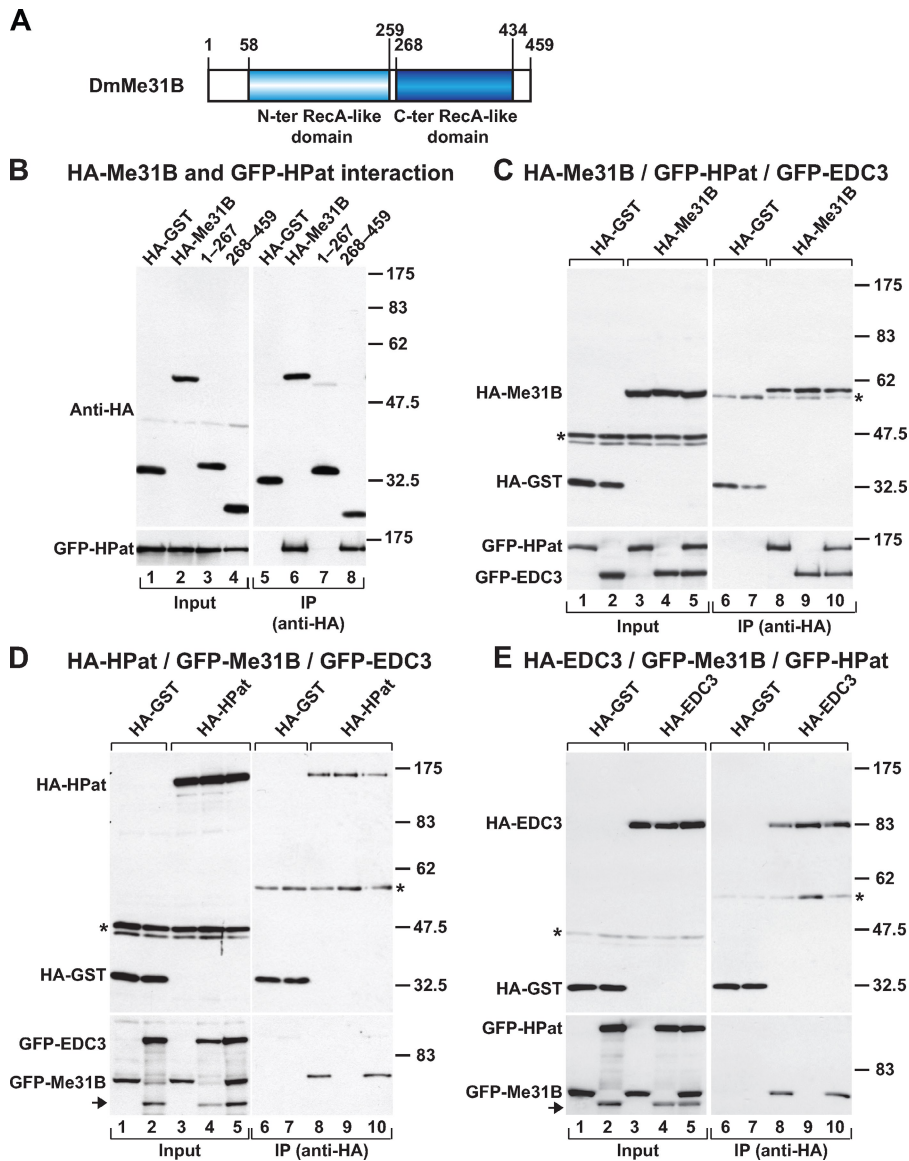
Figure 3. **HPat interacts with the C-terminal RecA-like domain of Me31B.** (A) Me31B consists of two RecA-like domains. Numbers above the protein outline represent amino acid positions at fragment boundaries for the *D. melanogaster* protein. N-ter, N-terminal; C-ter, C-terminal. (B) HA-tagged Me31B or the indicated Me31B protein fragments were coexpressed in S2 cells with GFP-HPat. Cell lysates were immunoprecipitated and analyzed as described in Fig. 1. (C–E) S2 cells were cotransfected with mixtures of three plasmids. In C, the plasmids encoded HA-Me31B, GFP-HPat, and GFP-EDC3; in D, the plasmids encoded HA-HPat, GFP-Me31B, and GFP-EDC3; in E, the mixture consisted of HA-EDC3, GFP-Me31B, and GFP-HPat. In all panels, HA-GST served as a negative control. Cell lysates were immunoprecipitated and analyzed as described in Fig. 1. Arrows indicate EDC3 or HPat protein degradation fragments. Asterisks indicate cross-reactivity of the primary antibodies with an endogenous protein (input panels) or of the secondary antibody with the immunoglobulin heavy chain (IP panels). (B–E) Molecular mass is indicated in kilodaltons.

The proline-rich region is required for P-body localization

HPat localizes to P bodies both in *S. cerevisiae* and in metazoa and is required for P-body integrity (Eulalio et al., 2007a,b; Parker and Sheth, 2007). This localization does not appear to be affected by a GFP tag (Fig. 6 A). Therefore, we sought to define which interactions are critical for HPat accumulation in P bodies by examining where HPat fragments localize. A fragment of HPat comprising the N-terminal conserved sequence and the proline-rich region localized to P bodies in 37% of the cell population (Fig. 6 B), whereas a fragment comprising the Mid domain and Pat-C, which interacts with DCP2 and the LSm1–7 ring, dispersed throughout the cytoplasm (Fig. 6 C). This suggests that the N-terminal fragment retains the ability to localize to P bodies, although not as efficiently as full-length HPat, which localized to P bodies in 87% of the cell population (Fig. 6 A).
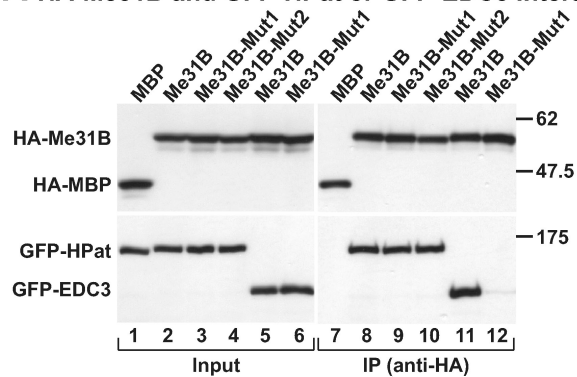
We next investigated whether the N-terminal conserved sequence or the proline-rich region were sufficient for P-body localization. A GFP fusion of the HPat N-terminal sequence,

which interacts with Me31B, spread throughout the cell (Fig. 6 D). Moreover, when overexpressed, this protein fusion affected the integrity of endogenous P bodies, significantly reducing them in number and size (Fig. 6 D). In contrast, the proline-rich region accumulated in P bodies in 47% of the cells (Fig. 6 E), suggesting that the proline-rich region is sufficient for P-body localization. In line with this interpretation, we found that an HPat mutant lacking the proline-rich region was evenly distributed throughout the cell (Fig. 6 F). Furthermore, the overexpression of this mutant affected the integrity of endogenous P bodies in a dominant-negative manner. We conclude that the proline-rich region of HPat plays a critical role in maintaining P-body integrity and promoting HPat accumulation in P bodies.

HPat promotes degradation of bound mRNAs

To better understand the function of HPat in decapping, we investigated whether binding of HPat to an mRNA was sufficient to promote degradation. To this end, we made use of the tethering

A HA-Me31B and GFP-HPat or GFP-EDC3 interaction

HA-Me31B
HA-MBP
GFP-HPat
GFP-EDC3

— 62
— 47.5
— 175

1 2 3 4 5 6 | 7 8 9 10 11 12
Input | IP (anti-HA)

B EDC3-FDF peptide competition

FDF ADA | FDF ADA

HA-Me31B
HA-MBP
GFP-HPat

— 62
— 47.5
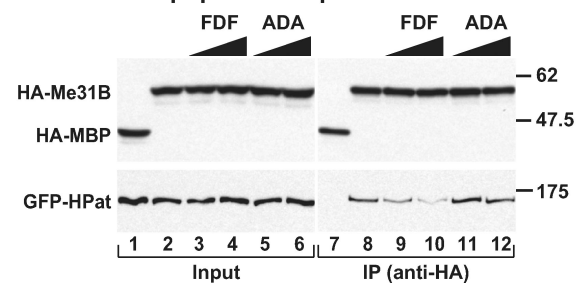— 175

1 2 3 4 5 6 | 7 8 9 10 11 12
Input | IP (anti-HA)

Figure 4. **Me31B establishes mutually exclusive interactions with HPat, EDC3, and Tral.** (A) HA-tagged Me31B or the indicated Me31B mutants were coexpressed in S2 cells with GFP-HPat or -EDC3. Cell lysates were immunoprecipitated and analyzed as described in Fig. 1. Me31B mutants carry alanine substitutions of the following residues: Gln281, His284, Tyr288, and Lys292 (Mut1) or Phe405, His408, Glu411, and Lys412 (Mut2). (B) HA-MBP or -Me31B was coexpressed with GFP-HPat in S2 cells. Cell lysates were immunoprecipitated using a monoclonal anti-HA antibody. In lanes 3–6 and 9–12, increasing amounts (5 and 20 µg) of purified recombinant EDC3-FDF peptide or of the corresponding ADA mutant were added to the cell lysates before IP as indicated. (A and B) Molecular mass is indicated in kilodaltons.

assay previously described (Gehring et al., 2005). This assay involves the expression of λN fusion proteins that bind with high affinity to five BoxB hairpins (5BoxB) in the 3′ untranslated region of a firefly luciferase (F-Luc) reporter mRNA (F-Luc–5BoxB reporter).

S2 cells were transiently transfected with the F-Luc–5BoxB reporter, a plasmid expressing HPat fused to the λN-HA peptide, and a plasmid encoding *Renilla* luciferase (R-Luc). As negative control, we used an inactive mutant of the Argonaute-1 protein (AGO1-F2V2) because this protein is comparable in size with HPat. Relative to cells expressing the AGO1-F2V2 mutant, tethered λN-HA–HPat reduced F-Luc activity 2.5-fold (Fig. 7 A). A stronger inhibitory effect was observed for GW182, which served as a positive control (Fig. 7 A; Behm-Ansmant et al., 2006).

To determine whether HPat inhibits F-Luc activity by repressing translation directly or indirectly by reducing mRNA levels, we analyzed by Northern blot the steady-state levels of the F-Luc–5BoxB mRNA. We found that λN-HA–HPat partially reduced reporter mRNA (Fig. 7, A and B [lane 3]) at a level that fully accounted for the decrease of F-Luc activity (Fig. 7 A, black vs. gray bars). HPat did not affect the expression of an F-Luc reporter lacking the BoxB elements (Fig. S1 E).

Together, these results indicate that HPat directs bound mRNAs to degradation.

The proline-rich region is required for HPat to degrade bound mRNAs

We next performed tethering assays using the aforementioned HPat deletion mutants. We observed that deleting the conserved N-terminal sequence, which interacts with Me31B, reduced HPat activity in the tethering assay (Fig. 7 A, ΔN-ter). In contrast, HPat mutants lacking either the Mid domain or Pat-C individually or simultaneously (Fig. 7, A and B, N-ter+P-rich) were fully active.

Unexpectedly, deleting the proline-rich region abolished HPat activity (Fig. 7, A and B, ΔP-rich). Conversely, the proline-rich region alone was more active than full-length HPat (Fig. 7, A and B, P-rich). All proteins were expressed at comparable levels (Fig. 7 C). We conclude that the proline-rich region is both necessary and sufficient to trigger degradation of bound mRNAs.

HPat triggers deadenylation and decapping

Given the role of HPat and orthologues in mRNA decapping, we next tested whether HPat-mediated mRNA degradation required the activity of decapping activators. To this end, we performed the tethering assay in cells codepleted of two decapping activators, DCP1 and EDC4. In such cells, decapping was efficiently inhibited, blocking mRNA degradation caused by tethered GW182 (Fig. 7, D and E [lane 2 vs. lane 1]). The accumulated transcripts were shorter, which is consistent with the observation that GW182 triggers mRNA deadenylation (Behm-Ansmant et al., 2006). We confirmed that these transcripts lack a poly(A) tail by oligo (dT)–targeted RNase H cleavage (Fig. 7 F). Specifically, in cells expressing λN-HA–AGO1-F2V2, both the F-Luc reporter and the endogenous rp49 mRNA (encoding ribosomal protein L32) migrated faster after oligo (dT)–directed RNase H cleavage had removed the poly(A) tail (Fig. 7 F, lane 2 vs. lane 1). In contrast, in cells expressing λN-HA–GW182, RNase H treatment did not affect F-Luc reporter mobility, indicating that it was already deadenylated (Fig. 7 F, lane 4 vs. lane 3).

Codepletion of DCP1 and EDC4 also prevented HPat-mediated degradation of the reporter, which accumulated both in the poly- and deadenylated form (Fig. 7, E [lane 3] and F [lane 6 vs. lane 5]). The polyadenylated form corresponded to the fraction of the mRNA that was not degraded by HPat (Fig. 7 B, lane 3). The accumulation of the deadenylated form indicates that HPat promotes deadenylation. This finding might explain why luciferase activity is not restored despite restoration of mRNA levels (Fig. 7 D) because deadenylated transcripts are translated less efficiently. Similar results were obtained for all HPat fragments containing the proline-rich region (Fig. 7, D and E).

We could not analyze the effect of codepleting DCP1 and EDC4 in cells expressing two HPat fragments (N-ter+P-rich and P-rich) because overexpressing these fragments had cytotoxic effects (i.e., low recovery of transfected cells). This was not observed in control cells, suggesting that in the background
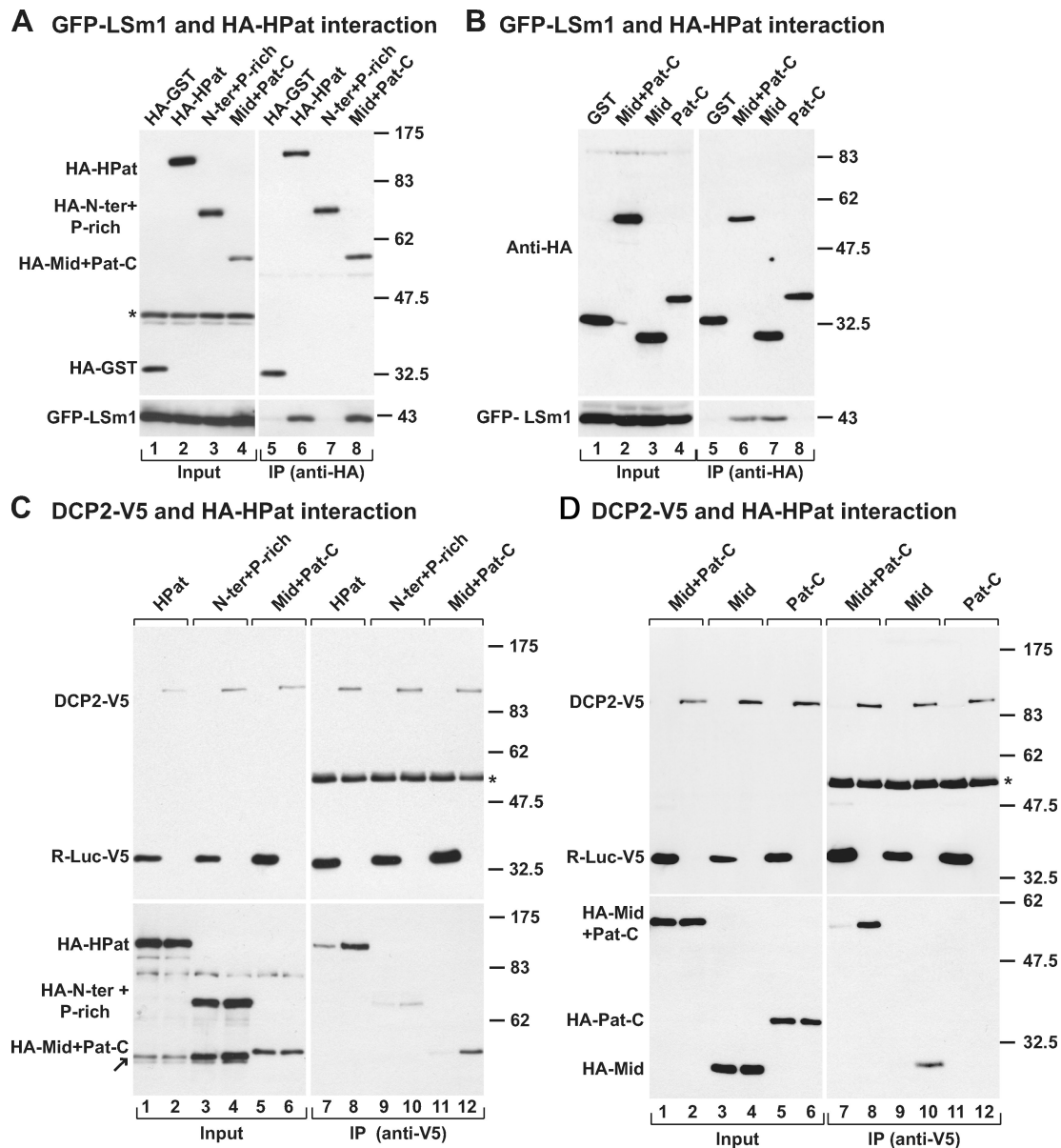
Figure 5. **The Mid domain and Pat-C interact with DCP2 and the LSm1–7 complex.** (A–D) Interaction between full-length HPat or HPat fragments with GFP-LSm1 or DCP2-V5. Protein interactions were analyzed as described in Fig. 1. Asterisks indicate cross-reactivity of the anti-HA antibody with an endogenous protein (input panels) or of the V5 antibody with the immunoglobulin heavy chain (IP panels). Note that in C, a degradation product arising from full-length HPat, an HPat fragment containing the N-terminal (N-ter) and proline-rich (P-rich) regions (in lanes 1–4), and the fragment containing the Mid domain and Pat-C (lanes 5 and 6) have a similar mobility (arrow). Molecular mass is indicated in kilodaltons.

of the double DCP1–EDC4 knockdown, these protein fragments are toxic.

To further demonstrate that HPat triggers deadenylation followed by decapping, we performed two independent experiments. First, we examined the F-Luc–5BoxB mRNA in cells expressing a dominant-negative mutant of DCP2 that strongly inhibits decapping in S2 cells partially depleted of endogenous DCP2. Again, in the presence of GW182 or HPat, the reporter accumulated in the deadenylated form, co-migrating with an F-Luc–5BoxB transcript lacking the poly(A) tail (Fig. 7 H).

In the second experiment, we exposed transfected cells to actinomycin D to inhibit transcription and then analyzed the levels of F-Luc–5BoxB mRNA over time (as compared with the long-lived rp49 mRNA, which has a half-life >8 h). In cells expressing the AGO1-F2V2 mutant, the half-life of F-Luc–5BoxB mRNA was ~2 h, whereas in cells expressing λN-HPat or the proline-rich region, the half-life of this mRNA was ~40 min or 10 min, respectively (Fig. 7 I). Importantly, in cells expressing HPat or the proline-rich region, the F-Luc–5BoxB transcripts accumulating 15–90 min after adding actinomycin D were deadenylated (Fig. 7 I). These results further demonstrate that HPat-mediated decay is initiated by deadenylation. Collectively, our results indicate that HPat triggers deadenylation followed by decapping of bound mRNAs and that these activities reside in the proline-rich region.

GFP-HPat (green) | Tral (red) | Merge

HPat
Full length — A 87%±10

N-ter+P-rich — B 37%±4 / 63%±4

Mid+Pat-C — C 97%±3

N-ter — D 99%±1

P-rich — E 47%±6 / 53%±6
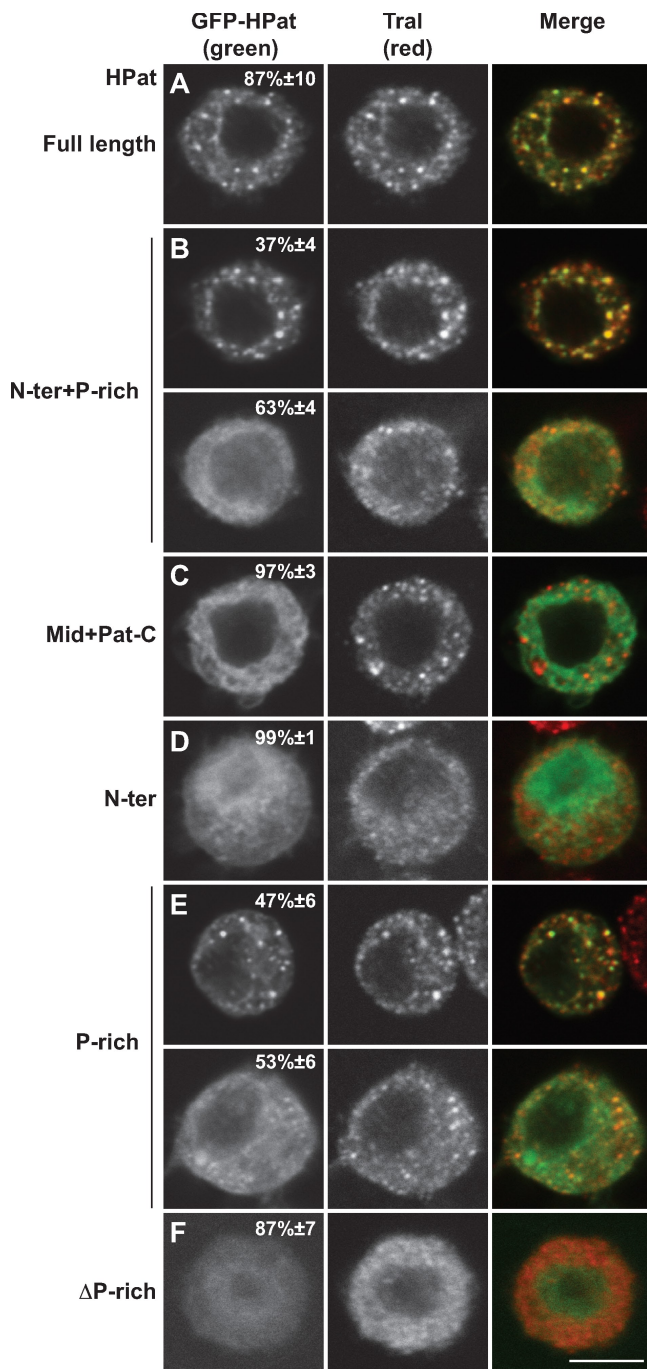
ΔP-rich — F 87%±7

Figure 6. **The proline-rich region is required for HPat accumulation in P bodies.** (A–F) Confocal fluorescent micrographs of fixed S2 cells expressing GFP-tagged fusions of full-length HPat or the protein fragments indicated on the left. Cells were stained with affinity-purified anti-Tral antibodies. The merged images show the GFP signal in green and the Tral signal in red. The fraction of cells exhibiting a staining identical to that shown in the representative panel was determined by scoring at least 100 cells per transfection in three independent transfections performed per protein. Mean values ± standard deviations are shown. N-ter, N-terminal; P-rich, proline-rich. Bar, 5 µm.

HPat interacts with components of the CCR4–NOT deadenylase complex

The finding that HPat triggers deadenylation followed by decapping of bound mRNA suggests that HPat interacts with components of the deadenylase complex. Accordingly, we observed that HPat coimmunoprecipitated components of the CCR4–NOT complex (including POP2, CCR4, NOT2, NOT3/5, and NOT4) in an RNA-independent manner (Fig. 8 A). These results suggest that HPat acts as an adaptor molecule, bridging the interaction between the deadenylation and decapping machineries. However, it is important to note that HPat is not required for deadenylation per se because depleting HPat causes deadenylated mRNAs to accumulate. Thus, in the absence of HPat, only decapping but not deadenylation is inhibited (Fig. 9; Eulalio et al., 2007c), which is in agreement with the results reported previously in yeast (Bouveret et al., 2000; He and Parker, 2001; Tharun and Parker, 2001).

To define the domains of HPat required for the interaction with CCR4–NOT deadenylase complex components, we performed co-IP assays with the aforementioned protein fragments. We observed that the Mid domain was both necessary and sufficient for HPat to interact with CCR4 (Fig. 8, B and C).

## The Mid domain and Pat-C are required for decapping in vivo

The tethering assay allows functional domains to be identified once HPat is artificially tethered to an mRNA, but additional domains may also be essential for HPat function because they mediate target binding. To further investigate the requirement for HPat domains in decapping, we established a complementation assay in which endogenous HPat was depleted using a double-stranded RNA (dsRNA) targeting HPat ORF. HPat fragments were then tested for their ability to restore decapping in HPat-depleted cells. Transcripts encoding the recombinant proteins were made resistant to the dsRNA by introducing mutations that disrupt base pair interactions with the dsRNA without altering the protein sequence.

To monitor decapping, we used the F-Luc–5BoxB reporter tethered to GW182. The GW182 triggers deadenylation of the F-Luc–5BoxB reporter, which is then decapped, and subsequently, the mRNA body is digested exonucleolytically (Fig. 7; Behm-Ansmant et al., 2006). Inhibiting decapping prevents mRNA degradation by GW182, and so deadenylated decay intermediates accumulate (Fig. 7 E, lane 2 vs. lane 1). Therefore, the accumulation of the deadenylated F-Luc–5BoxB mRNA reflects a block in decapping.

As shown in Fig. 9 A, tethered λN-HA–GW182 reduces mRNA levels threefold relative to that measured in cells expressing the λN-HA peptide alone. Depleting HPat did not significantly restore reporter mRNA levels (unpublished data). This result was expected because we previously showed that at least two decapping activators must be codepleted in S2 cells to inhibit decapping (Eulalio et al., 2007c).

We then tested whether we could inhibit decapping of the F-Luc–5BoxB reporter in cells depleted of HPat plus EDC4, DCP1, or Me31B and whether decapping could be restored by expressing a dsRNA-resistant form of HPat. To our surprise, although all combinations inhibited decapping, the dsRNA-resistant form of HPat restored decapping only in cells codepleted of HPat and Me31B (Fig. 9 B, lane 4 vs. lane 2). These observations indicate that, in this context and/or for this reporter, the HPat–Me31B interaction is dispensable for decapping.
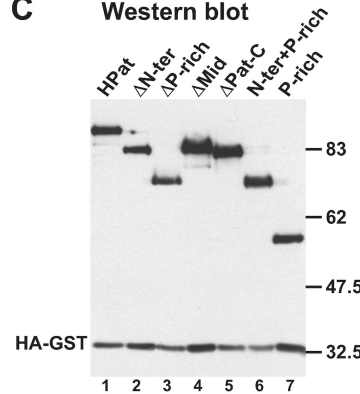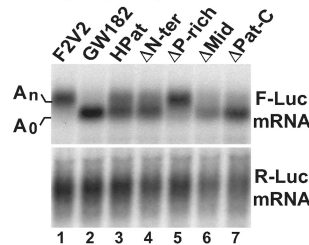
A F-Luc-5BoxB reporter in control cells
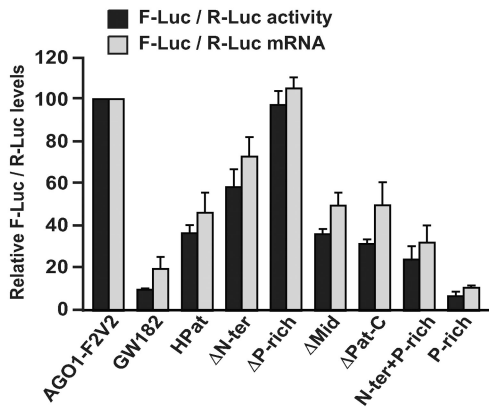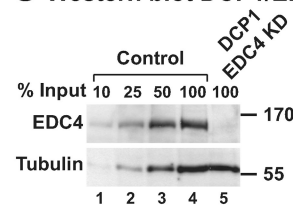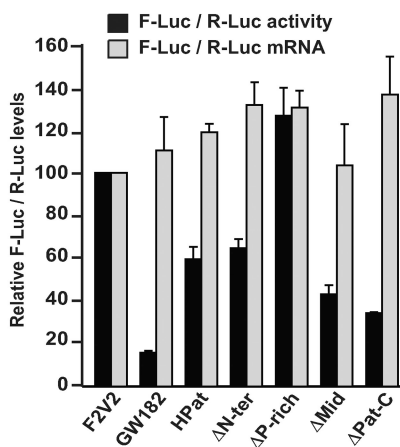
B Control cells

C Western blot

D F-Luc-5BoxB reporter in DCP1/EDC4 KD
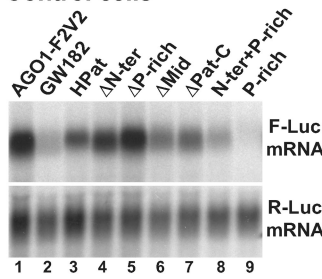
E DCP1/EDC4 KD

F RNase H

G Western blot DCP1/EDC4 KD
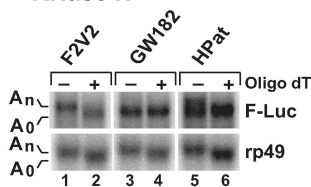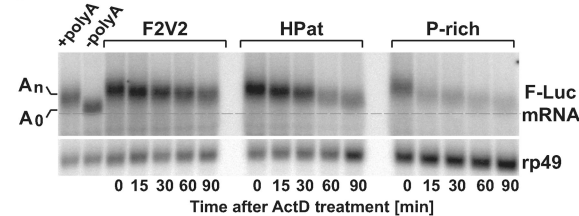
H
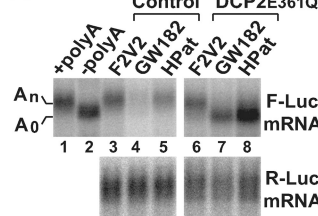
I

Figure 7. **HPat triggers deadenylation and decapping of bound mRNAs.** (A–F) Control S2 cells (treated with GFP dsRNA) or cells codepleted of DCP1 and EDC4 were transfected with a mixture of three plasmids, one expressing the F-Luc–5BoxB reporter, another expressing R-Luc, and a third expressing λN-HA–AGO1-F2V2 (negative control) or λN-HA fusions of wild-type HPat or fragments, as indicated. F-Luc activity and mRNA levels were normalized to those of the *Renilla* and set to 100 in cells expressing λN-HA–AGO1-F2V2. Mean values ± standard deviations from three independent experiments are shown. B and E show Northern blot analysis of representative RNA samples shown in A and D, respectively. (C) Full-length HPat and fragments were expressed at comparable levels. (F) RNA samples shown in E (lanes 1–3) were treated with RNase H in the absence or presence of oligo (dT) and analyzed by Northern blot. rp49 mRNA served as a positive control for the RNase H treatment. (G) Western blot analysis of control and DCP1–EDC4-depleted cell lysates. α-Tubulin served as a loading control. KD, knockdown. (C and G) Molecular mass is indicated in kilodaltons. (H) Tethering assay in cells expressing a dominant-negative mutant of DCP2 (E361Q). In lanes 1 and 2, samples isolated from cells expressing poly- and unadenylated F-Luc–5BoxB mRNA served as size markers. (I) S2 cells were transfected as described in A. 3 d after transfection, cells were treated with 5 μg/ml actinomycin D (ActD) and harvested at the indicated time points. The dashed line indicates the position of the deadenylated decay intermediate. N-ter, N-terminal; P-rich, proline-rich.

We next tested whether HPat mutants could restore reporter mRNA degradation in the background of the double Me31B–HPat knockdown. Here, the HPat mutant lacking the Me31B-binding sequence restored mRNA degradation (Fig. 9 B, lane 6), which is consistent with a study in *S. cerevisiae* showing that deleting the N-terminal sequence of Pat1 only modestly affects decapping (Pilkington and Parker, 2008).

Unlike results obtained in yeast (Pilkington and Parker, 2008), in our experiments, mRNA degradation was not restored

by HPat mutants lacking Pat-C alone or in combination with the Mid domain, indicating that Pat-C is also required for decapping in vivo (Fig. 9, B [lanes 12 and 14] and C). Moreover, deleting the proline-rich region or the Mid domain also impaired decapping (Fig. 9, B [lanes 8 and 10] and C). Finally, expressing the proline-rich region alone was not sufficient to restore decapping (Fig. 9, B [lane 16] and C). All proteins were expressed at comparable levels and had no dominant-negative effects when expressed in control cells (Fig. 9, A and E). Thus, with the
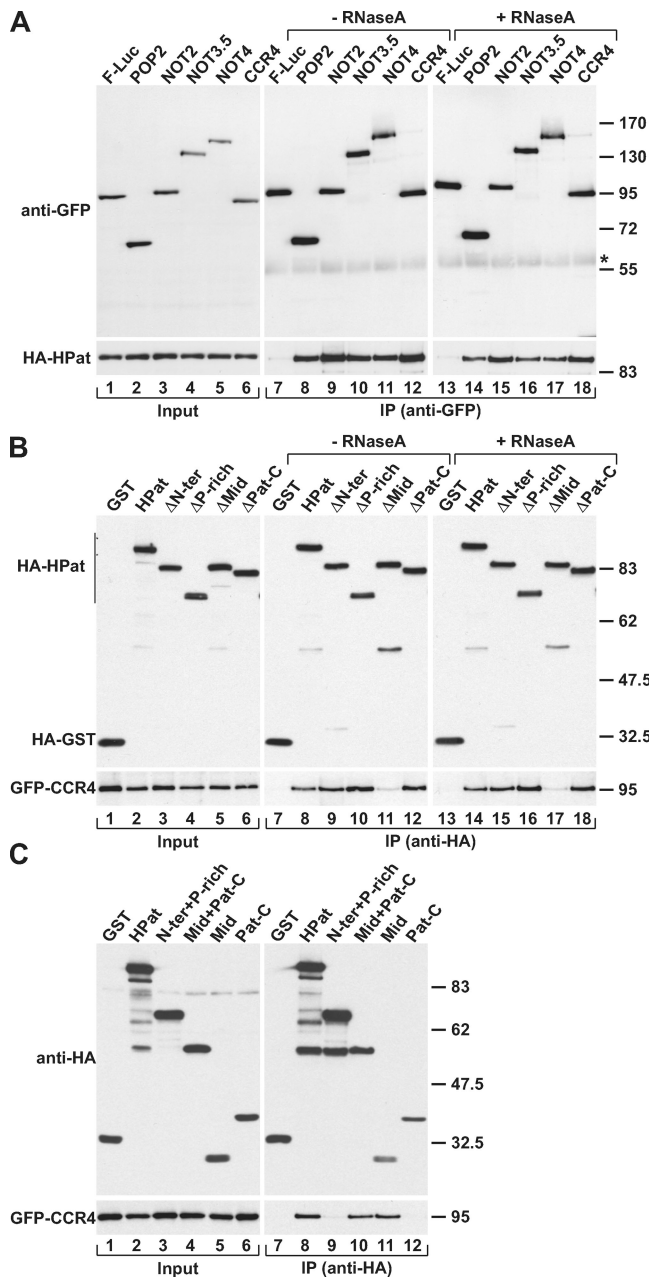
Figure 8. **HPat interacts with components of the CCR4–NOT complex.** (A–C) Interaction between HA-HPat wild type or mutants and GFP-tagged components of the CCR4–NOT complex. In lanes 13–18 of A and B, cell lysates were treated with RNase A before IP. F-Luc–GFP (A) or HA-GST (B and C) served as negative controls. The asterisk indicates cross-reactivity of the secondary antibody with the immunoglobin heavy chain. Molecular mass is indicated in kilodaltons. N-ter, N-terminal; P-rich, proline-rich.

HPat, previous studies showing that wild-type Pat1 coimmunoprecipitates a variety of yeast mRNAs (Tharun et al., 2000; Tharun and Parker, 2001). We used real-time quantitative RT-PCR (RT-qPCR) to analyze the levels of an F-Luc mRNA reporter coimmunoprecipitating with HPat and observed that HA-HPat coimmunoprecipitated the F-Luc reporter 10-fold more efficiently than did HA-GST, which served as a background control for the IPs (Fig. 10 A). Furthermore, an HPat mutant lacking Pat-C was partially impaired in the association with the reporter mRNA, whereas deleting the Mid domain abolished association with the F-Luc mRNA (Fig. 10 A). All proteins were present in the immunoprecipitates at comparable levels (Fig. 10 B). Thus, the Mid domain, which interacts with the LSm1–7 ring, CCR4, and DCP2, is required for HPat recruitment to mRNAs. This activity is likely stimulated by the contribution of Pat-C.

In yeast, Pat1 has been reported to associate with mRNAs via LSm1-dependent and -independent mechanisms and to exhibit RNA-binding activity (Tharun and Parker, 2001; Pilkington and Parker, 2008). Accordingly, we observed that HPat association with the F-Luc reporter was not affected in cells depleted of LSm1 (Fig. 10, A and B). These results suggest that HPat could be recruited to mRNA targets via a redundant mechanism, including the interaction with the deadenylase complex, the interaction with the LSm1–7 ring, or direct RNA binding.
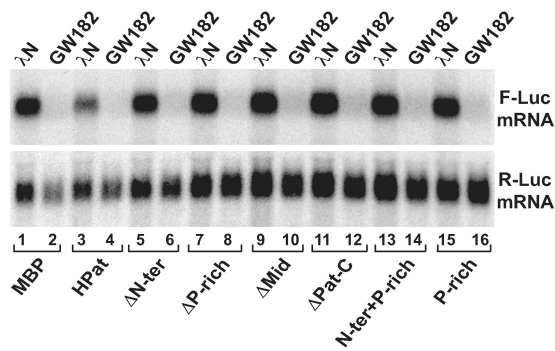
Discussion

Decapping of eukaryotic mRNAs depends on prior deadenylation, which ensures that functional, polyadenylated mRNAs are not decapped prematurely. However, little is known regarding the mechanisms that promote decapping of deadenylated mRNAs in vivo. In this study, we show that the protein HPat coimmunoprecipitates with decapping factors, including DCP2, Me31B, and the LSm1–7 ring as well as components of the CCR4–NOT deadenylase complex. These findings suggest that HPat acts as a bridging factor between the deadenylation and decapping machineries. Furthermore, the HPat proline-rich region is necessary and sufficient to trigger deadenylation and decapping of bound mRNAs. However, in addition to the proline-rich region, both the Mid domain and Pat-C are required to restore decapping in cells depleted of endogenous HPat. Finally, we show that the Mid domain and Pat-C are required for HPat recruitment to mRNAs. Therefore, our work suggests a model whereby HPat associates with mRNAs undergoing deadenylation via interactions with the deadenylase complex or the LSm1–7 ring; subsequently, HPat recruits decapping factors, thereby committing deadenylated mRNAs to degradation through the 5′ to 3′ mRNA decay pathway.

HPat interacts with decapping activators and the CCR4–NOT deadenylase complex

In this study, we show that in *D. melanogaster* cells, HPat coimmunoprecipitates Me31B, DCP2, the LSm1–7 ring, and components of the CCR4–NOT deadenylase complex (Fig. 10 C). We mapped the domains on HPat that mediate these interactions

exception of the N-terminal sequence, all domains of HPat contribute to decapping in vivo.

HPat recruitment to mRNAs is mediated by the Mid domain and Pat-C

The Mid domain and Pat-C were not required for HPat to promote mRNA degradation in tethering assays but were required for decapping in complementation assays, so we speculate that these domains contribute to target mRNA binding. To investigate this possibility, we confirmed and extended, for
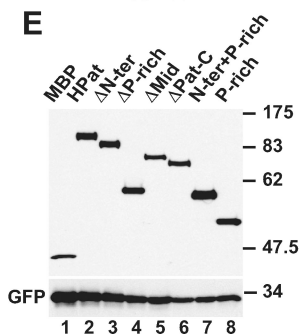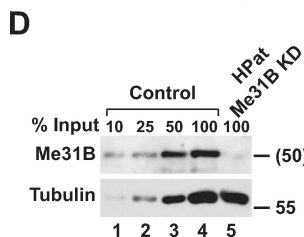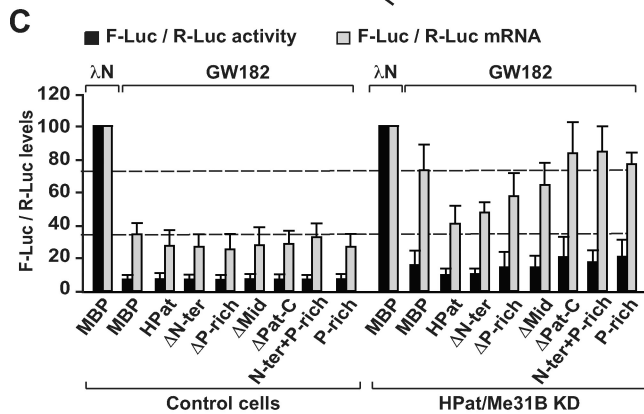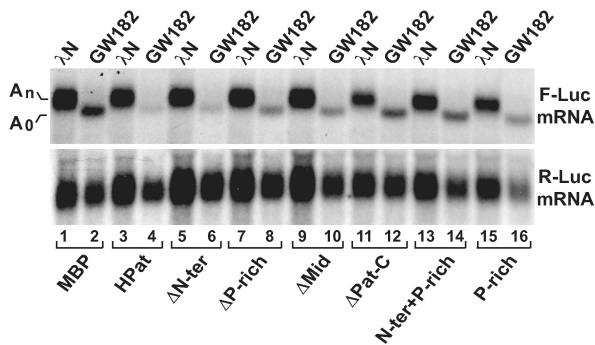
Figure 9. **Complementation assay.** (A–E) Control S2 cells (treated with GFP dsRNA) or cells codepleted of HPat and Me31B were cotransfected with a mixture of three plasmids, one expressing the F-Luc–5BoxB reporter, another expressing λN-HA–GW182 or the λN-HA peptide, and a third expressing R-Luc. Plasmids (5 ng) expressing HA-MBP, wild-type HA-HPat, or fragments (lacking the λN tag) were included in the transfection mixtures, as indicated. RNA samples were analyzed by Northern blot. (C) F-Luc activity and mRNA levels were normalized to that of the R-Luc. For each condition, the normalized values of F-Luc activity and mRNA levels were set to 100 in control cells expressing the λN-HA peptide and HA-MBP. Mean values ± standard deviations from three independent experiments are shown. Dashed lines indicate F-Luc–5BoxB mRNA levels in

and showed that the Mid domain is required for HPat to interact with CCR4 and the LSm1–7 ring. Similarly, in *S. cerevisiae*, the corresponding region of Pat1 confers binding to the LSm1–7 ring (Pilkington and Parker, 2008). Moreover, the Mid domain cooperates with Pat-C to mediate DCP2 binding, suggesting that DCP2 binds HPat independently of the LSm1–7 ring. Future experiments will unravel whether HPat binds decapping and deadenylation factors simultaneously or consecutively and whether these interactions are direct.

We also show that a conserved N-terminal sequence of HPat interacts with the C-terminal RecA-like domain of Me31B. Surprisingly, this conserved sequence is dispensable for HPat activity in complementation assays, suggesting that mRNAs targeted for GW182-dependent degradation are efficiently decapped even when HPat and Me31B do not interact directly. However, the HPat–Me31B interaction may play a role in decapping mRNAs degraded by pathways distinct from the microRNA pathway.

An important observation is that HPat also interacted with components of the CCR4–NOT deadenylase complex. Because HPat is not required for deadenylation per se (Eulalio et al., 2007c; this study), an interaction with the CCR4–NOT complex most likely plays a role in recruiting HPat to mRNAs undergoing deadenylation, providing a mechanism to couple decapping to the removal of the mRNA poly(A) tail.

Me31B is part of at least three distinct protein complexes

Previously, we showed that Me31B interacts with EDC3 and Tral to form distinct protein complexes (Tritschler et al., 2009). This study shows that a third complex exists, consisting minimally of Me31B, HPat, and the LSm1–7 ring. The interaction between Me31B and HPat is also detected in yeast (Coller et al., 2001; Fischer and Weis, 2002); however, our study revealed that EDC3, Tral, and HPat compete for binding to Me31B. Thus, Me31B establishes mutually exclusive interactions with EDC3, Tral, and HPat. The ability of Me31B and orthologues to establish mutually exclusive interactions with multiple partners provides a mechanistic explanation for the myriad functions performed by this protein and further supports the idea that Me31B and its orthologues act as remodeling subunits in diverse protein complexes (Tritschler et al., 2009). The role of these complexes in posttranscriptional mRNA regulation (e.g., decapping or translational repression) is specified by the additional components.

The proline-rich region is required for P-body assembly and mRNA decapping

In this study, we show that the proline-rich region of HPat promotes deadenylation and decapping of bound RNAs and is required for P-body localization, indicating that this region

cells expressing MBP and GW182. (D) Western blot analysis of control and HPat–Me31B-depleted cell lysates. α-Tubulin served as a loading control. (E) Full-length HPat and fragments were expressed at comparable levels. (D and E) Molecular mass is indicated in kilodaltons. KD, knockdown; N-ter, N-terminal; P-rich, proline-rich.
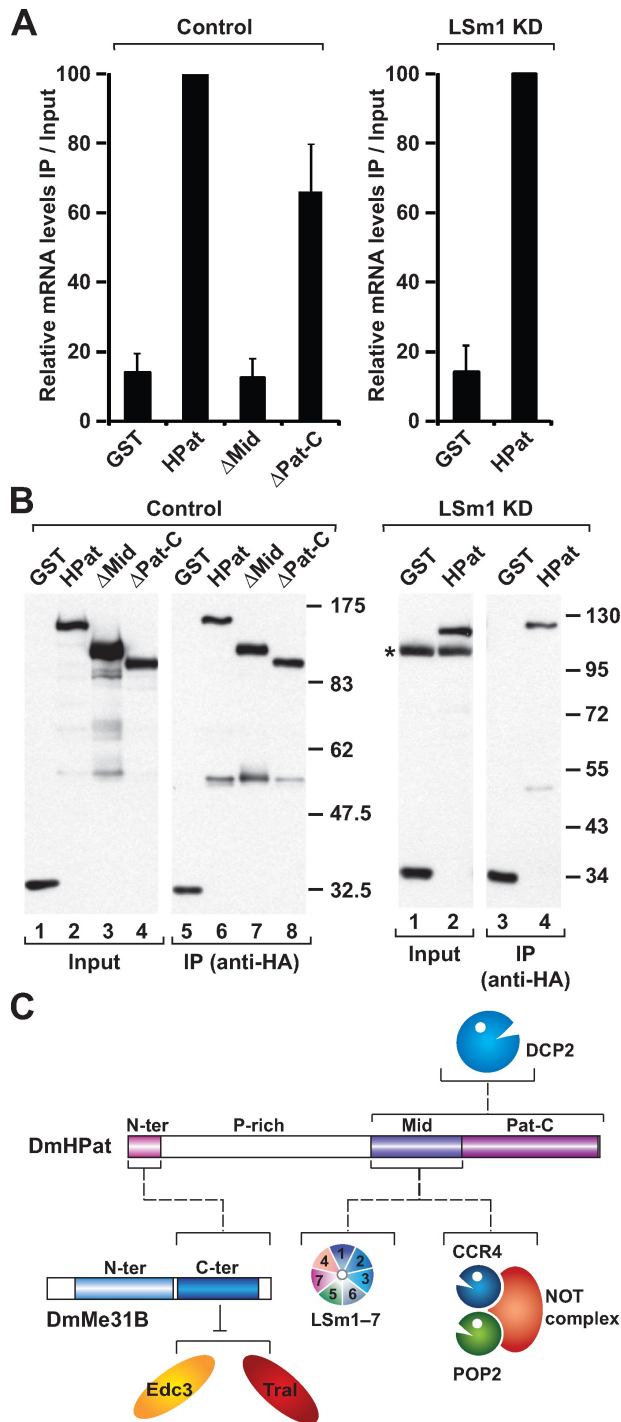
Figure 10.   **The Mid domain is required for HPat recruitment to mRNA targets.** (A) Control or LSm1-depleted S2 cells were transfected with a mixture of three plasmids, one expressing an F-Luc reporter, another expressing HA-GST, wild-type HA-HPat, or mutants, and a third plasmid expressing R-Luc. Cell lysates were immunoprecipitated using an anti-HA antibody. The levels of the F-Luc reporter in the immunoprecipitates (IP) were analyzed by RT-qPCR and normalized to the corresponding input sample. Mean values ± standard deviations from four independent experiments are shown. (B) The efficacy of the IPs was examined by Western blotting. Molecular mass is indicated in kilodaltons. (C) Schematic model summarizing the protein interactions described in this study. KD, knockdown; N-ter, N-terminal; P-rich, proline-rich.

interacts with additional components of the mRNA decay pathway. However, in IP assays, the proline-rich region was dispensable for HPat interaction with decapping factors or deadenylase complex components, suggesting that the binding partners of this region remain to be identified.

How can a proline-rich region mediate such diverse activities? Proline residues could play a structural role by keeping this region in an extended conformation, rendering short sequence motifs accessible for interaction with protein partners. In addition, proline-rich regions can also provide multiple, nonspecific binding sites for protein–protein interactions, thereby contributing to the assembly of multiprotein complexes (Williamson, 1994).

P-body components often contain low-complexity Q/N-rich regions proposed to facilitate P-body formation via self-association or association with Q/N-rich domains on other proteins (Decker et al., 2007; Mazzoni et al., 2007; Reijns et al., 2008). These regions are often rich in proline in addition to or instead of glutamine. The region of *D. melanogaster* HPat required for P-body localization is rich in proline and glutamine; however, the length and composition of this region varies among Pat1 orthologues from different species, suggesting that the physical interactions between decapping activators that are critical for P-body localization may not be conserved. This view is supported by evidence from *S. cerevisiae* in which Pat-C but not the proline-rich region is required for Pat1 to accumulate in P bodies (Pilkington and Parker, 2008).

The Mid domain is required for HPat binding to mRNAs

In addition to the proline-rich region, we show that the Mid domain and Pat-C are required to restore decapping in cells depleted of endogenous HPat. However, the Mid domain and Pat-C are dispensable for mRNA degradation when HPat is artificially tethered to an mRNA. One possible explanation for this difference is that the reporters used in these assays are decapped through distinct mechanisms. An alternative but not mutually exclusive explanation is that the Mid domain and Pat-C play a role in target binding and therefore are no longer required once HPat is tethered to an mRNA. Consistent with this second possibility, we show that the Mid domain is essential for HPat to associate with mRNAs. The Mid domain may interact with mRNAs indirectly, via the LSm1–7 ring, as shown in yeast (Tharun and Parker, 2001; Chowdhury and Tharun, 2008, 2009). However, our results indicate that HPat can associate with mRNAs in LSm1-depleted cells, suggesting that HPat binds RNA either directly or through other interacting partners (e.g., the CCR4–NOT complex). In agreement with this, in *S. cerevisiae*, both the Mid domain and Pat-C exhibit RNA-binding activity (Pilkington and Parker, 2008).

What role might the Pat-C domain play in decapping? In *S. cerevisiae*, it exhibits RNA-binding activity. Accordingly, in *D. melanogaster* S2 cells, this domain contributes to target mRNA binding. However, the absolute requirement for this domain in complementation assays suggests that it may have additional functions in mRNA decapping.

A role for HPat in mediating the deadenylation dependence of decapping

Our findings suggest that in vivo HPat facilitates the deadenylation dependence of decapping. Several lines of evidence support this assertion. First, HPat may be preferentially recruited to deadenylated mRNAs because it associates with the LSm1–7 ring, a protein complex which binds oligoadenylated mRNAs preferentially (Tharun and Parker, 2001; Chowdhury and Tharun, 2008, 2009). In addition, we found that components of the deadenylase complex interact with HPat, suggesting that HPat is recruited to mRNAs actively undergoing deadenylation. Once recruited, the association between HPat and decapping factors will promote the assembly of decapping complexes in cis, committing deadenylated mRNAs to degradation via the 5′ to 3′ mRNA decay pathway.

Materials and methods

DNA constructs
Luciferase reporters and plasmids for the expression of GFP- or λN-HA–tagged cDNAs encoding full-length AGO1-F2V2, DCP1, DCP2, EDC3, EDC4, GW182, LSm1, LSm3, LSm7, Me31B, and Tral were described previously (Eulalio et al., 2007b; Tritschler et al., 2007, 2008, 2009). A plasmid for the expression of HA-XRN1 was obtained by inserting the XRN1 ORF into the Not1 and Xba1 sites of pAc5.1–λN-HA vector. A plasmid for the expression of DCP2-V5 was obtained by inserting the DCP2 ORF into the EcoRV and Xho1 sites of pAc5.1A, in frame with the V5 epitope. Plasmids for the expression of HA- or GFP-tagged HPat were obtained by inserting the HPat ORF into the EcoRV and Not1 sites of pAc5.1–λN-HA and pAc5.1-EGFP vectors. HPat fragments were cloned into the pAc5.1–λN-HA and pAc5.1-EGFP vectors. For the complementation assay shown in Fig. 9, the λN tag was deleted, and cDNAs were made resistant to HPat dsRNA, which targets mRNA sequences encoding aa 743–968 of HPat. Plasmids for the expression of deadenylase complex components were obtained by inserting the corresponding cDNAs in the pAc5.1–λN-EGFP vector using the restriction sites EcoRV–Not1 (POP2, which is related to CAF1), EcoR1–Not1 (CCR4), HindIII–XbaI (NOT2), HindIII–Not1 (NOT3/5), and XhoI–BstBI (NOT4).

Co-IP assays, Western blotting, and fluorescence microscopy
Transfections were performed in 6-well dishes using Effectene transfection reagent (QIAGEN). Protein co-IPs, Western blotting, and immunofluorescence were performed as described previously (Tritschler et al., 2007, 2008, 2009). For co-IPs, cells were collected 3 d after transfection, washed with PBS, and lysed for 15 min on ice in NET buffer (50 mM Tris, pH 7.4, 150 mM NaCl, 1 mM EDTA, and 0.1% Triton X-100) supplemented with protease inhibitors. Cells were spun at 16,000 g for 15 min at 4°C. Anti-HA (Covance) or anti-GFP antibodies were added to the supernatants (2.5 μl/2 × 10⁶ cells). After 1 h at 4°C, 25 μl of protein G–agarose (Roche) were added, and the mixtures were rotated for 1 h at 4°C. Beads were washed three times with NET buffer and once with NET buffer without Triton X-100. Bound proteins were eluted with sample buffer. Proteins were separated by SDS-PAGE and transferred to nitrocellulose membranes. Membranes were blocked in PBS containing 5% fat-free milk powder and 0.3% Tween 20. Western blotting was performed with polyclonal anti-HA antibodies (1:1,000; Sigma-Aldrich) or anti-GFP antibodies (1:2,000), using the CDP-Star chemiluminescent immunoblot system (Western-Star kit; Tropix), as recommended by the manufacturer.

For immunofluorescence, S2 cells were allowed 15 min to adhere to poly-D-lysine–coated coverslips and fixed with 2% paraformaldehyde for 10 min. Cells were then permeabilized with 0.1% Triton X-100 in PBS (10 min) and stained with an affinity-purified anti-Tral antibody diluted 1:250 in PBS containing 1% BSA (1 h). Alexa Fluor 594–labeled goat anti–mouse antibody (Invitrogen) was used at a dilution of 1:1,000. Cells were mounted using Fluoromount-G (SouthernBiotech). Images were acquired at room temperature using a confocal microscope (TCS SP2; Leica) fitted with a Plan-Apochromat 100× NA 1.40 oil immersion objective and a series of three photomultipliers (Hamamatsu Photonics) controlled with the Leica confocal software (version 2.61). Images were prepared using Photoshop (Adobe).

Tethering and complementation assays
RNA interference was performed as described previously (Eulalio et al., 2007c). For the λN-tethering assay, the following plasmids were cotransfected:

0.1 μg reporter plasmid (F-Luc–5BoxB or F-Luc), 0.4 μg pAc5.1–R-Luc as transfection control, and 0.025 μg of plasmids expressing λN-HA–protein fusions. For the complementation assay, cells were depleted on days 0 and 4, transfected on day 6, and collected on day 9. The transfection mixtures contained 0.1 μg reporter plasmid (F-Luc–5BoxB), 0.4 μg pAc5.1–R-Luc as transfection control, and 0.1 μg of plasmids expressing the λN-HA peptide or λN-HA–GW182. When indicated, 0.005 μg of plasmids expressing wild-type HPat or HPat fragments was cotransfected. HA–maltose-binding protein (MBP) served as a negative control. In all experiments, cells were collected 3 d after transfection. F-Luc and R-Luc activities were measured using the Dual-Luciferase reporter assay system (Promega). Northern blotting was performed as described previously (Behm-Ansmant et al., 2006). RNase H (USB) digestion using a (dT)₁₅ oligonucleotide was performed according to the manufacturer's instructions.

Reverse transcription and RT-qPCR
The interaction of HPat with mRNAs was tested as described by Zekri et al. (2009). In these experiments, the transfection mixtures contained 0.3 μg of an F-Luc reporter plasmid, 0.2 μg of the *Renilla* transfection control, and 0.5 μg of plasmid expressing full-length HPat or fragments or HA-GST. S2 cells (10–12 × 10⁶ cells) were collected 3 d after transfection, washed with PBS, and lysed in 0.5 ml of NET buffer (50 mM Tris, pH 7.4, 150 mM NaCl, 1 mM EDTA, and 0.1% NP-40) supplemented with protease inhibitors. Cells were lysed by three 30-s sonications, followed by a 15-min incubation on ice. Cells were spun at 16,000 g for 15 min at 4°C. Anti-HA antibodies were added to the cleared lysates (2.5 μl/2 × 10⁶ cells). After 1 h at 4°C, aliquots (1/10) of the cleared lysates (input) were kept aside for both RNA extraction and Western blotting analysis, and 20 μl of protein G–agarose was added to the remaining lysate. Before addition to the lysates, protein G–agarose beads were preincubated with 0.5 mg of yeast RNA and 30 μg BSA for 1 h at 4°C. Lysates were rotated with protein G–agarose beads for 1 h at 4°C. Beads were washed four times with NET buffer and once with NET buffer and eluted with 60 μl of 2× SDS-PAGE protein sample buffer. 40 μl of the eluate was used for RNA analysis. RNA was prepared from input and immunoprecipitates using TRIZOL-LS reagent (Invitrogen) according to the manufacturer's protocol. DNase treatment was performed using the TURBO DNA-free kit (Applied Biosystems) for 30 min at 37°C. RNAs were detected via cDNA synthesis and real-time quantitative PCR. cDNAs were synthesized with M-MuLV reverse transcription (Fermentas) and the F-Luc reporter–specific primer 5′-TGTTTACATAACCG-GACATAATCA-3′, according to the manufacturer's protocols. Quantitative PCR analysis was performed using gene-specific primer pairs (as indicated below) and SYBR green PCR master mix (Applied Biosystems). Each sample was analyzed in triplicate. mRNA levels in the immunoprecipitates were normalized to the respective input levels. Primer sequences for F-Luc reporter are 5′-GGCCGAAGACGCCAAAAACATAAAG-3′ (forward) and 5′-AATAACGCGCCCAACACCGGCA-3′ (reverse).

Online supplemental material
Fig. S1 shows that HPat interacts with LSm1 and DCP2 in an RNA-independent manner. Fig. S2 shows that HPat and Tral interact with Me31B in a mutually exclusive manner. Online supplemental material is available at http://www.jcb.org/cgi/content/full/jcb.200910141/DC1.

References

Bail, S., and M. Kiledjian. 2006. More than 1 + 2 in mRNA decapping. *Nat. Struct. Mol. Biol.* 13:7–9. doi:10.1038/nsmb0106-7

Behm-Ansmant, I., J. Rehwinkel, T. Doerks, A. Stark, P. Bork, and E. Izaurralde. 2006. mRNA degradation by miRNAs and GW182 requires both CCR4:NOT deadenylase and DCP1:DCP2 decapping complexes. *Genes Dev.* 20:1885–1898. doi:10.1101/gad.1424106

Bonnerot, C., R. Boeck, and B. Lapeyre. 2000. The two proteins Pat1p (Mrt1p) and Spb8p interact in vivo, are required for mRNA decay, and are functionally linked to Pab1p. *Mol. Cell. Biol.* 20:5939–5946. doi:10.1128/MCB.20.16.5939-5946.2000

Bouveret, E., G. Rigaut, A. Shevchenko, M. Wilm, and B. Séraphin. 2000. A Sm-like protein complex that participates in mRNA degradation. *EMBO J.* 19:1661–1671. doi:10.1093/emboj/19.7.1661

Chowdhury, A., and S. Tharun. 2008. lsm1 mutations impairing the ability of the Lsm1p-7p-Pat1p complex to preferentially bind to oligoadenylated RNA affect mRNA decay in vivo. *RNA.* 14:2149–2158. doi:10.1261/rna.1094208

Chowdhury, A., and S. Tharun. 2009. Activation of decapping involves binding of the mRNA and facilitation of the post-binding steps by the Lsm1-7-Pat1 complex. *RNA.* 15:1837–1848. doi:10.1261/rna.1650109

Chowdhury, A., J. Mukhopadhyay, and S. Tharun. 2007. The decapping activator Lsm1p-7p-Pat1p complex has the intrinsic ability to distinguish between oligoadenylated and polyadenylated RNAs. *RNA.* 13:998–1016. doi:10.1261/rna.502507

Coller, J., and R. Parker. 2005. General translational repression by activators of mRNA decapping. *Cell.* 122:875–886. doi:10.1016/j.cell.2005.07.012

Coller, J.M., M. Tucker, U. Sheth, M.A. Valencia-Sanchez, and R. Parker. 2001. The DEAD box helicase, Dhh1p, functions in mRNA decapping and interacts with both the decapping and deadenylase complexes. *RNA.* 7:1717–1727. doi:10.1017/S135583820101994X

Decker, C.J., D. Teixeira, and R. Parker. 2007. Edc3p and a glutamine/asparagine-rich domain of Lsm4p function in processing body assembly in *Saccharomyces cerevisiae. J. Cell Biol.* 179:437–449. doi:10.1083/jcb.200704147

Eulalio, A., I. Behm-Ansmant, and E. Izaurralde. 2007a. P bodies: at the crossroads of post-transcriptional pathways. *Nat. Rev. Mol. Cell Biol.* 8:9–22. doi:10.1038/nrm2080

Eulalio, A., I. Behm-Ansmant, D. Schweizer, and E. Izaurralde. 2007b. P-body formation is a consequence, not the cause, of RNA-mediated gene silencing. *Mol. Cell. Biol.* 27:3970–3981. doi:10.1128/MCB.00128-07

Eulalio, A., J. Rehwinkel, M. Stricker, E. Huntzinger, S.-F. Yang, T. Doerks, S. Dorner, P. Bork, M. Boutros, and E. Izaurralde. 2007c. Target-specific requirements for enhancers of decapping in miRNA-mediated gene silencing. *Genes Dev.* 21:2558–2570. doi:10.1101/gad.443107

Fischer, N., and K. Weis. 2002. The DEAD box protein Dhh1 stimulates the decapping enzyme Dcp1. *EMBO J.* 21:2788–2797. doi:10.1093/emboj/21.11.2788

Fromont-Racine, M., A.E. Mayes, A. Brunet-Simon, J.C. Rain, A. Colley, I. Dix, L. Decourty, N. Joly, F. Ricard, J.D. Beggs, and P. Legrain. 2000. Genome-wide protein interaction screens reveal functional networks involving Sm-like proteins. *Yeast.* 17:95–110. doi:10.1002/1097-0061(20000630)17:2<95::AID-YEA16>3.0.CO;2-H

Gehring, N.H., J.B. Kunz, G. Neu-Yilik, S. Breit, M.H. Viegas, M.W. Hentze, and A.E. Kulozik. 2005. Exon-junction complex components specify distinct routes of nonsense-mediated mRNA decay with differential cofactor requirements. *Mol. Cell.* 20:65–75. doi:10.1016/j.molcel.2005.08.012

Hatfield, L., C.A. Beelman, A. Stevens, and R. Parker. 1996. Mutations in transacting factors affecting mRNA decapping in *Saccharomyces cerevisiae. Mol. Cell. Biol.* 16:5830–5838.

He, W., and R. Parker. 2001. The yeast cytoplasmic LsmI/Pat1p complex protects mRNA 3′ termini from partial degradation. *Genetics.* 158:1445–1455.

Houseley, J., J. LaCava, and D. Tollervey. 2006. RNA-quality control by the exosome. *Nat. Rev. Mol. Cell Biol.* 7:529–539. doi:10.1038/nrm1964

Mazzoni, C., I. D'Addario, and C. Falcone. 2007. The C-terminus of the yeast Lsm4p is required for the association to P-bodies. *FEBS Lett.* 581:4836–4840. doi:10.1016/j.febslet.2007.09.009

Parker, R., and U. Sheth. 2007. P bodies and the control of mRNA translation and degradation. *Mol. Cell.* 25:635–646. doi:10.1016/j.molcel.2007.02.011

Pilkington, G.R., and R. Parker. 2008. Pat1 contains distinct functional domains that promote P-body assembly and activation of decapping. *Mol. Cell. Biol.* 28:1298–1312. doi:10.1128/MCB.00936-07

Reijns, M.A., R.D. Alexander, M.P. Spiller, and J.D. Beggs. 2008. A role for Q/N-rich aggregation-prone regions in P-body localization. *J. Cell Sci.* 121:2463–2472. doi:10.1242/jcs.024976

Scheller, N., P. Resa-Infante, S. de la Luna, R.P. Galao, M. Albrecht, L. Kaestner, P. Lipp, T. Lengauer, A. Meyerhans, and J. Díez. 2007. Identification of PatL1, a human homolog to yeast P body component Pat1. *Biochim. Biophys. Acta.* 1773:1786–1792. doi:10.1016/j.bbamcr.2007.08.009

Simon, E., S. Camier, and B. Séraphin. 2006. New insights into the control of mRNA decapping. *Trends Biochem. Sci.* 31:241–243. doi:10.1016/j.tibs.2006.03.001

Tharun, S. 2009. Lsm1-7-Pat1 complex: a link between 3′ and 5′-ends in mRNA decay? *RNA Biol.* 6:228–232. doi:10.4161/rna.6.3.8282

Tharun, S., and R. Parker. 2001. Targeting an mRNA for decapping: displacement of translation factors and association of the Lsm1p-7p complex on deadenylated yeast mRNAs. *Mol. Cell.* 8:1075–1083. doi:10.1016/S1097-2765(01)00395-1

Tharun, S., W. He, A.E. Mayes, P. Lennertz, J.D. Beggs, and R. Parker. 2000. Yeast Sm-like proteins function in mRNA decapping and decay. *Nature.* 404:515–518. doi:10.1038/35006676

Tritschler, F., A. Eulalio, V. Truffault, M.D. Hartmann, S. Helms, S. Schmidt, M. Coles, E. Izaurralde, and O. Weichenrieder. 2007. A divergent Sm fold in EDC3 proteins mediates DCP1 binding and P-body targeting. *Mol. Cell. Biol.* 27:8600–8611. doi:10.1128/MCB.01506-07

Tritschler, F., A. Eulalio, S. Helms, S. Schmidt, M. Coles, O. Weichenrieder, E. Izaurralde, and V. Truffault. 2008. Similar modes of interaction enable Trailer Hitch and EDC3 to associate with DCP1 and Me31B in distinct protein complexes. *Mol. Cell. Biol.* 28:6695–6708. doi:10.1128/MCB.00759-08

Tritschler, F., J.E. Braun, A. Eulalio, V. Truffault, E. Izaurralde, and O. Weichenrieder. 2009. Structural basis for the mutually exclusive anchoring of P body components EDC3 and Tral to the DEAD box protein DDX6/Me31B. *Mol. Cell.* 33:661–668. doi:10.1016/j.molcel.2009.02.014

Williamson, M.P. 1994. The structure and function of proline-rich regions in proteins. *Biochem. J.* 297:249–260.

Wyers, F., M. Minet, M.E. Dufour, L.T. Vo, and F. Lacroute. 2000. Deletion of the PAT1 gene affects translation initiation and suppresses a PAB1 gene deletion in yeast. *Mol. Cell. Biol.* 20:3538–3549. doi:10.1128/MCB.20.10.3538-3549.2000

Zekri, L., E. Huntzinger, S. Heimstädt, and E. Izaurralde. 2009. The silencing domain of GW182 interacts with PABPC1 to promote translational repression and degradation of microRNA targets and is required for target release. *Mol. Cell. Biol.* 29:6220–6231. doi:10.1128/MCB.01081-09